Available online at www.sciencedirect.com
ScienceDirect
Journal of Photochemistry and Photobiology A: Chemistry 185 (2007) 1–12
Journal of Photochemistry and Photobiology A:Chemistry
www.elsevier.com/locate/jphotochem

Spectral properties and G-quadruplex DNA binding selectivities of a series of unsymmetrical perylene diimides

Haluk Dincalp [a,*], Nesibe Avcıbası [b,c], Sıddık Icli [b,*]

[a] *Department of Chemistry, Faculty of Art and Science, Celal Bayar University, Muradiye 45030 Manisa, Turkey*
[b] *Solar Energy Institute, Ege University, Bornova, 35100 Izmir, Turkey*
[c] *Ege Vocational Training School, Ege University, Bornova, 35100 Izmir, Turkey*

Received 19 February 2006; received in revised form 25 April 2006; accepted 26 April 2006
Available online 7 May 2006

Abstract

A series of new unsymmetrical perylene diimides have been synthesized to investigate their binding selectivities to G-quadruplex DNA structure, a unique four-stranded DNA motif, which is significant to the regulation of telomerase activity. The structures of the perylene diimides have been characterized by IR spectrophotometer, ^{1}H NMR, ^{13}C NMR, MS, TGA and time-resolved instruments. Spectrochemical behaviors have been investigated by visible absorption and fluorescence emission spectra. The spectral characterization of the compounds has been investigated in five common organic solvents of different polarity and in water (in 170 mM phosphate buffer at pH 6). Marked red shifts of absorbance and fluorescence emission bands of the compounds in aqueous solution are compared with the other organic solutions. The fluorescence quantum yields are determined low in more polar solvents and also calculated to be about less than about 0.05 in aqueous solution because of the aggregation effects. Photodegradation rate constants (k_p) of the synthesized compounds have been compared under xenon lamp irradiation in acetonitrile solution.

Binding abilities of the synthesized perylene diimides to different form of DNA strands have been investigated by visible absorption and fluorescence spectroscopy in the phosphate buffer solutions. Also, pH-dependent aggregation and G-quadruplex DNA binding selectivity of these ligands have been compared. Among these ligands, *N*-(2,6-diisopropylphenyl)-*N*′-(4-pyridyl)-perylene-3,4,9,10-tetracarboxylic diimide (PYPER) has been found to be the most selective interactive ligand for G-quadruplex formed in the G4′-DNA structure. PYPER has shown a significant selectivity to G4′-DNA which is comprised of d(TTAGGG) repeats, known as human telomeres, in the phosphate buffer at pH 6. The absorption maximum of the PYPER/G4′-DNA complex has given bathochromic shift of 7 nm with respect to the absorption maximum of DNA-free solution of PYPER in phosphate buffer at pH 6. Fluorescence quenching experiments between PYPER and G4′-DNA show that PYPER demonstrates about a 9.3-fold selectivity for binding to G4′-DNA versus ds-DNA base pairs with the bimolecular rate constant of 0.95×10^{12} M^{-1} s^{-1}.

Keywords: Perylene diimide; Fluorescence quenching; G-quadruplex DNA; Human telomerase; Anti-cancer agent

1. Introduction

Symmetrical and unsymmetrical perylene diimides (PDIs) and their related structure perylene monoimides present a target of considerable current interest in biological as well as electronic areas for many decades. PDIs are mostly used in electrical and optical applications, such as field-effect transistors [1], photovoltaic applications as a n-type semiconductor system [2–4], dye lasers technology [5], electrophotographic devices [6], organic light-emitting diodes [7] and photorefractive thin film technology [8]. Due to their great photo and thermal stabilities under visible light irradiation and fairly high quantum yield ($\Phi_f \approx 1$) in the common organic solvents [9,10], they are drawn much attention for being used as sensitizers and photocatalysts in photosynthetic applications [11]. Besides their conventional uses in high technology applications, PDIs are a one of key ligands in photodynamic therapy [12], and also G-quadruplex DNA stabilization and inhibition of telomerase activity in cancer cells [13–15]. In photodynamic therapies, PDIs produce active oxygen species, which initiate the oxidation of cancer cells under visible light irradiation. There has been currently great interest

* Corresponding authors. Tel.: +90 232 3886025; fax: +90 232 3886027.
E-mail addresses: haluk.dincalp@bayar.edu.tr (H. Dincalp), siddik.icli@ege.edu.tr (S. Icli).

1010-6030/$ – see front matter © 2006 Elsevier B.V. All rights reserved.
doi:10.1016/j.jphotochem.2006.04.035

in exploring the potential of G-quadruplex DNA binding selectivity of PDI dyes. This selectivity has crucial point of inhibition of human telomerase, which is responsible for growth of cancer cells.

Most cancer cells have a high level of enzyme telomerase. This enzyme, which is expressed in 80–90% of all tumor cells is lacking in most normal cells [16]. Telomerase has the ability to add DNA back to the telomeres, and to accelerate the uncontrolled growth of tumor cells [17–19]. Telomeres are composed mostly of guanosines. The last few guanosines at the end of each telomere can fold into a sort of box, called a G-quadruplex. DNA quadruplexes comprise stacked tetrads, each of which arises from planar association of four guanosines in a cyclic Hoogsteen hydrogen bonding arrangement [20,21]. The ability of telomere DNA to adopt the G-quadruplex structure in the laboratory studies is so well established that many researchers believe not only in the existence of these structures inside cells but also in their essential role in maintaining the integrity of the telomeres. The box-like G-quadruplex structures at the end of chromosomes are thought to be the knot that prevents the chromosomes from unraveling. Many groups have designed and synthesized some molecular structures, which are believed to interact with G-quadruplex DNA structures to play an important role to maintain the telomeres [22–26]. One of the commonly preferred and employed compounds in the G-quadruplex DNA binding studies is PDIs.

A number of water-soluble PDI derivatives with different side chains have been synthesized and studied as a ligand to interact with the G-quadruplex structure [27–33]. Also, in experiments to understand how PDI ligands interact or bind to G-quadruplex DNA structures, a set of NMR titrations of *N*,*N*′-bis[2-(1-piperidino)ethyl]-3,4,9,10-perylenetetracarboxylic diimide (PIPER) in solutions of G-quadruplexes related to human telomeric DNA have shown strong binding of the ligand to the G-quadruplex DNA structure. The binding site of the ligand to G-quadruplex DNA is the aromatic core of the ligand, but the side chain of the ligand PIPER plays an important role in the binding affinity. NMR titration experiments have shown that in the case of the human telomeres containing a d(TTAGGG) sequence, the ligand PIPER is located between terminal G4 planes. In the longer telomeric sequences, the ligand is bound at the GT step by a threading intercalation mode [13]. All the G-quadruplex interactive PDI ligands mentioned in the literature are symmetrical perylene diimide derivatives. None of the articles has shown concern for the G-quadruplex DNA binding selectivity of unsymmetrical PDI ligands. According to the absorption and emission measurements in this study, unsymmetrical structures of PDIs have evidently shown some specific interactions with the G-quadruplex DNA structures. The absorption maxima of the compounds complexed with quadruplex DNA are shifted to the longer wavelengths as compared to the uncomplexed forms of the compounds. Also, fluorescence quenching measurements have indicated that aggregation kinetics of PDIs onto the DNA strands is responsible for the emission decrease or increase.

The present paper represents the results of the study of interaction of three unsymmetrical PDIs with five different forms of DNA strands in phosphate buffer at pH 6. The basic goal is to understand how unsymmetrical PDI ligands interact with the G-quadruplex DNA structure and to investigate the quadruplex binding selectivity and affinity of these unsymmetrical forms of PDI. The first part presents the photophysical and photochemical properties of the newly synthesized unsymmetrical PDI derivatives (Scheme 1) in five solvents of different polarity using steady state and time-resolved fluorescence experiments. The second part presents the binding selectivity of unsymmetrical PDI dyes to G-quadruplexes. The five oligonucleotides are used for determining the G-quadruplex DNA binding selectivity of the synthesized ligands. These oligonucleotides are single-stranded DNA (ss-DNA) [d(TTTTTT)], double-stranded-DNA (ds-DNA) $[d(CGCGCGATATCGCGCG)]_2$, intermolecular G-quadruplex DNA (G4-DNA) $[d(TAGGGTTA)]_4$, intramolecular G-quadruplex DNA (G4′-DNA) $[d(TTAGGG)_4]$ and dimeric hairpin quadruplex DNA (hp-DNA) $[d(GGGGTTTTGGGG)]_2$. DNA G-quadruplex structures are shown in Scheme 2.

2. Experimental

Perylene-3,4,9,10-tetracarboxylic dianhydride was purchased from Merck. Reactive amine compounds, including 2,6-diisopropylaniline, 4-aminopyridine, 1,4-phenylenediamine and *N*,*N*-dimethyl-*p*-phenylenediamine were received from Aldrich company. Quinoline, *tert*-butanol and all the solvents (methanol, *n*-hexane, ethyl acetate, chloroform, ethanol, tetrahydrofuran, toluene, acetonitrile, acetic acid), which were used in the synthetic applications were received from Merck. However, solvents used in spectroscopic and fluorimetric studies were of spectrophotometric grade. Imidazole was received from Fluka. All other chemicals (hydrochloric acid, sodium carbonate, potassium hydroxide pellet, zinc acetate dihydrate, potassium chloride, KH_2PO_4, $Na_2HPO_4{\cdot}12H_2O$, EDTA) were purchased from domestic chemical market.

^{1}H NMR and ^{13}C NMR spectra were measured on a 400 MHz Bruker spectrometer. The FT-IR spectra were determined on a Perkin-Elmer model Spectrum BX spectrophotometer by dispersing samples in KBr disks. The mass fragmentation of the compounds was realized with a DIP-mass technique on a Finnigan TSQ-700 (Thermoquest) spectrometer. The thermal properties of the synthesized ligands were measured on a Perkin-Elmer Thermogravimetric Analyzer Pyris 6 TGA instrument under nitrogen atmosphere with 4.5 bar gas pressure. The samples were held for 1 min at an initial temperature of 50 °C and, then heated to 1000 °C at a heating rate of 20 °C/min.

UV–visible spectra were obtained with a JASCO V-530 UV–vis spectrophotometer. Fluorescence spectra were recorded on a PTI QM1 fluorescence spectrophotometer. Fluorescence quantum yields of the synthesized unsymmetrical PDIs in organic solvents and an aqueous solution at pH 6 were calculated with reference to fluorescence emission of perylene-3,4,9,10-tetracarboxylic-bis-*N*,*N*′-dodecyl diimide (N-DODEPER) ($\Phi_f = 1.0$ in chloroform) which was synthesized as described previously [34]. The fluorescence decays of the ligands in toluene were taken with a sub-nanosecond pulsed LEDs. The system consisted of a pulsed laser driver and inter-

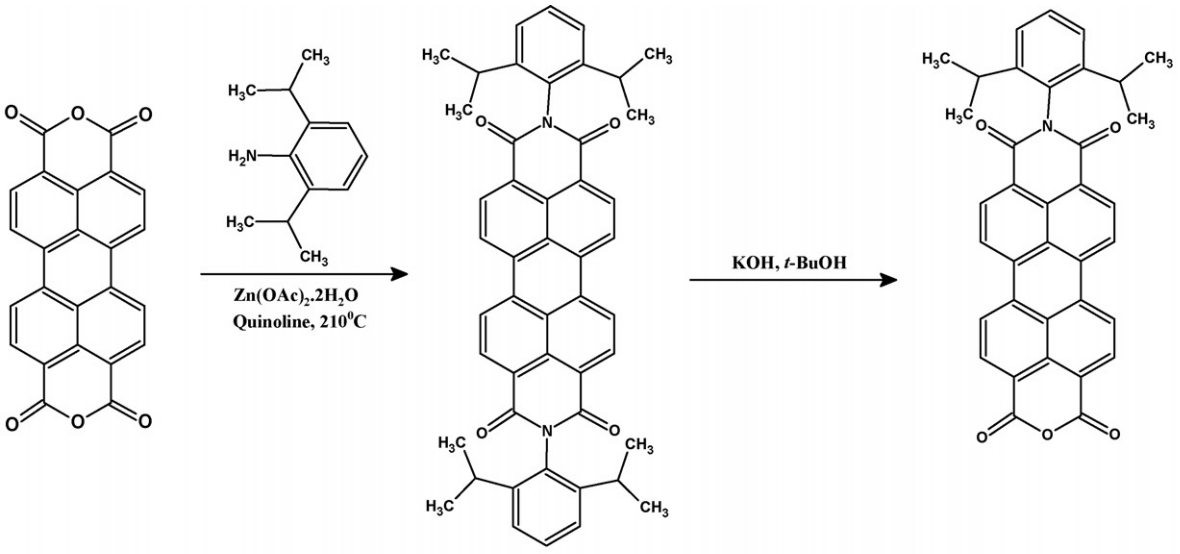

S1 S2

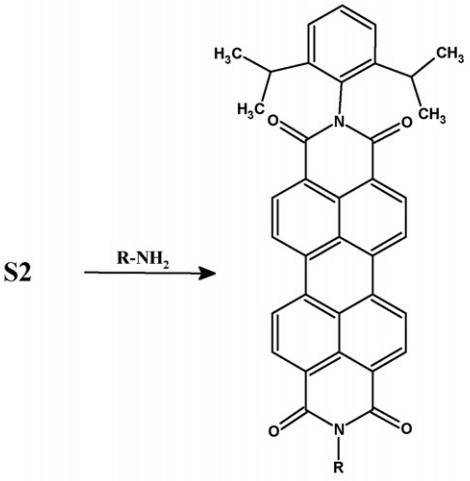

R= 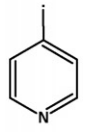

N-(2,6-diisopropylphenyl)-N'-(4-pyridyl)-perylene-3,4,9,10-tetracarboxylic diimide (**PYPER**)

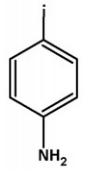

N-(2,6-diisopropylphenyl)-N'-(4-aminophenyl)-perylene-3,4,9,10-tetracarboxylic diimide (**ANPER**)

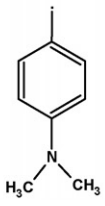

N-(2,6-diisopropylphenyl)-N'-[4-(N,N-dimethylaminophenyl)]-perylene-3,4,9,10-tetracarboxylic diimide (**DMANPER**)

Scheme 1. The synthesis of unsymmetrical PDIs (PYPER, ANPER and DMANPER).

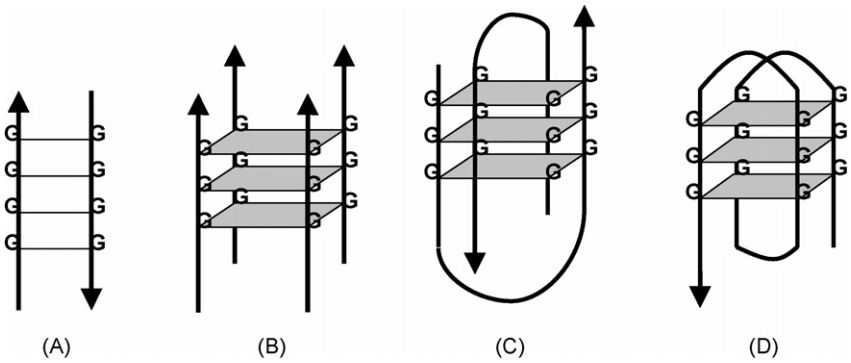

Scheme 2. Schematic representation of different forms of G-quadruplex DNA: (A) double-stranded-DNA (ds-DNA), (B) intermolecular G-quadruplex DNA (G4-DNA), (C) intramolecular G-quadruplex DNA (G4′-DNA) and (D) dimeric hairpin quadruplex DNA (hp-DNA).

changeable LED heads. LED heads with center wavelengths of 460 nm were available and could be provided with optional spectral bandpass filters to excite samples with a narrow spectral range. The fluorescence decay histograms were recorded in 2893 channels and the fluorescence decays were analyzed by using a Marquardt Algorithm [35] with a multiexponential fluorescence decay fit (FluoFit) software. The quality of the fits was judged by the fitting parameters, such as $\chi^2 < 1.2$ as well as by visual inspection of the residuals and autocorrelation function [36]. The instrument response function (IRF) was measured using a ludox scattering solution. All measurements were performed in 1 cm optical path length cuvettes. All the compounds were analyzed at an optical density of below 0.1.

2.1. Synthesis

2.1.1. N,N′-bis-(2,6-diisopropylphenyl)-perylene-3,4,9,10-tetracarboxylic diimide (S1)

S1 was synthesized according to the literature procedure [37]. A mixture of 3.14 mL (15 mmol) of 2,6-diisopropylaniline and 0.33 g (1.5 mmol) of $Zn(CH_3COO)_2{\cdot}2H_2O$ was added into a solution of 0.59 g (1.5 mmol) of perylene-3,4,9,10-tetracarboxylic dianhydride in 20 mL of quinoline. The mixture was stirred at 210 °C for 14 h under a nitrogen atmosphere. After cooling to room temperature, the mixture was added into 400 mL of methanol/10% hydrochloric acid (v/v = 2:1) under stirring. The solid precipitate was filtered off and stirred in 100 mL of cold Na_2CO_3 solution (10%) for 2 h. Then the precipitate was filtered again and washed with water until the filtrate was colorless. The solid was dried under vacuum at 90 °C for 16 h and purified by silica gel column chromatography with *n*-hexane/ethyl acetate (70:30) as eluent. Yield: 68%, mp > 300 °C. FT-IR (KBr, cm^{-1}): 2963, 2873, 1706 and 1667 (imide group), 1597, 1404, 1345, 1255, 1200, 959, 833, 813, 746 cm^{-1}. ^1H NMR ($CDCl_3$, δ 7.26 ppm): δ = 8.78 and 8.73 (8H, dd, perylene H); 7.50 (2H, t); 7.36 (4H, d); 2.75 (4H, h); 1.17 (24H, d) ppm.

2.1.2. N-(2,6-diisopropylphenyl)perylene-3,4,9,10-tetracarboxylic 3,4-anhydride 9,10-imide (S2)

A similar synthetic procedure given in the literature was followed for the synthesis of S2 [38]. A mixture of 0.28 g (0.4 mmol) of S1 ligand, 0.08 g (1.2 mmol) of 85% KOH pellets, and 15 mL of *tert*-BuOH was stirred at reflux for 15 h. The mixture was poured into a solution of 15 mL of AcOH and 7 mL of 2N HCl. The precipitate was washed with water and dried under vacuum at 80 °C for 16 h. Purification was accomplished by column chromatography on silica with chloroform/acetic acid (95:05) as eluent. Yield: 55%, mp > 300 °C. FT-IR (KBr, cm^{-1}): 2969, 2868, 1776 and 1737 (anhydride group), 1709 and 1667 (imide group), 1591, 1359, 1297, 1244, 1121, 1020, 811, 735 cm^{-1}. ^1H NMR ($CDCl_3$, δ 7.26 ppm): δ = 8.85 (2H, d, perylene H), 8.75 (2H, d, perylene H) and 8.71 (4H, d, perylene H); 7.55 (1H, t); 7.38 (2H, d); 2.69 (2H, h); 1.17 (12H, d) ppm.

2.1.3. N-(2,6-diisopropylphenyl)-N′-(4-pyridyl)-perylene-3,4,9,10-tetracarboxylic diimide (PYPER)

PYPER was prepared by the reaction of 0.100 g (0.18 mmol) of S2 compound with 0.034 g (0.36 mmol) of 4-aminopyridine in 5.5 mL of quinoline in the presence of 0.012 g (0.05 mmol) of $Zn(CH_3COO)_2{\cdot}2H_2O$. The mixture was stirred under a nitrogen atmosphere at 180 °C for 16 h. After cooling to room temperature the mixture was added into 30 mL of 2N HCl to precipitate the product, which was collected by filtration. The crude product was washed with 30 mL of cold Na_2CO_3 solution (10%) under vacuum, and then dried under vacuum at 90 °C for 16 h. The solid was passed through a silica column ($CHCl_3$:MeOH/92:08). Yield: 57%, mp > 300 °C. FT-IR (KBr, cm^{-1}): 2957, 2924, 1709 and 1664 (imide group), 1591, 1493, 1401, 1345, 1253, 1174, 808, 746 cm^{-1}. ^1H NMR ($CDCl_3$, δ 7.26 ppm): δ = 8.90 (2H, d, perylene H), 8.78 (2H, d, perylene H), 8.76 (2H, d, perylene H) and 8.73 (2H, d, perylene H); 7.53 (1H, t); 7.36 (2H, d); 7.45 (2H, d); 7.42 (2H, d); 2.74 (2H, h); 1.17 (12H, d) ppm. ^{13}C NMR [$CDCl_3$ δ 77 ppm (3 peaks); *d*-TFA δ 162 ppm (4 peaks), 115 ppm (4 peaks)]: 165 (C = O), 163 (C = O), 120–145 (aromatic C), 29 ($CH(CH_3)_2$), 23 ($CH(CH_3)_2$) ppm. DIP-mass: $[M]^+$ = 627 molecular ion peak; 584 $[M]^{\bullet+} - CH(CH_3)_2$; 467 $[M]^{\bullet+} - Ph\text{-}CH(CH_3)_2$; 398 $[M]^{\bullet+} - (CO)_2N\text{-}Ph\text{-}CH(CH_3)_2$.

2.1.4. N-(2,6-diisopropylphenyl)-N′-(4-aminophenyl)-perylene-3,4,9,10-tetracarboxylic diimide (ANPER)

A mixture of 0.100 g (0.18 mmol) of S2 compound, 0.392 g (3.62 mmol, 20 mol equivalent) of 1,4-phenylenediamine and

0.012 g (0.05 mmol) of $Zn(CH_3COO)_2{\cdot}2H_2O$ in 6 mL of quinoline was heated to 220 °C for 20 h under nitrogen gas protection. The mixture was cooled to room temperature and precipitated by adding to the solution of 30 mL of 2N HCl. The residue was filtrated under vacuum, and the filtrate was washed with 150 mL of Na_2CO_3 solution (10%) under vacuum until the green fluorescent color of the solution was disappeared. The solid was dried under vacuum at 90 °C for 16 h. Then, the $CHCl_3$/MeOH (90:10) system eluted the title compound. Yield: 70%, mp > 300 °C. FT-IR (KBr, cm^{-1}): 3361 and 3226 (amino group), 2963, 2873, 1703 and 1661 (imide group), 1591, 1513, 1353, 1250, 1177, 1124, 811, 746 cm^{-1}. ^1H NMR ($CDCl_3$, δ 7.26 ppm): δ = 8.73 (2H, d, perylene H), 8.69 (2H, d, perylene H), 8.67 (2H, d, perylene H) and 8.65 (2H, d, perylene H); 7.64 (1H, t); 7.46 (2H, d); 7.43 (2H, d); 7.27 (2H, d); 4.22 (2H, s); 2.68 (2H, h); 1.12 (12H, d) ppm. ^{13}C NMR [$CDCl_3$ δ 77 ppm (3 peaks); *d*-TFA δ 162 ppm (4 peaks), 115 ppm (4 peaks)]: 165 (C=O), 164 (C=O), 122–145 (aromatic C), 29 ($CH(CH_3)_2$), 23 ($CH(CH_3)_2$) ppm. DIP-mass: $[M]^{\bullet+}$ = 641 molecular ion peak was not observed, but 546 $[M]^{\bullet+}$ − Ph-NH_2; 531 $[M]^{\bullet+}$ − Ph-NH_2 − CH_3; 516 $[M]^{\bullet+}$ − Ph-NH_2 − $2CH_3$; 460 $[M]^{\bullet+}$ − Ph-NH_2 − $2CH(CH_3)_2$; 388 $[M]^{\bullet+}$ − Ph-$CH(CH_3)_2$ − Ph-NH_2; 316 $[M]^{\bullet+}$ − $(CO)_2$N-Ph-$CH(CH_3)_2$ − Ph-NH_2.

2.1.5. N-(2,6-diisopropylphenyl)-N′-[4-(N,N-dimethylaminophenyl)]-perylene-3,4,9,10-tetracarboxylic diimide (DMANPER)

Following a standard procedure, a mixture of 0.100 g (0.18 mmol) of S2, 0.074 g (0.54 mmol) *N*,*N*-dimethyl-*p*-phenylenediamine and 1.034 g imidazole was heated to 130 °C for 2 h in the glycerine bath under nitrogen gas protection. The warm solution was poured into 50 mL of ethanol. The solution was stirred with 50 mL of 2N HCl at room temperature for 2 h. The residue was filtrated and dried under vacuum at 100 °C for 14 h. Elution with ($CHCl_3$:MeOH/92:08) afforded the title compound. Yield: 72%, mp > 300 °C. FT-IR (KBr, cm^{-1}): 2957, 2873, 1703 and 1658 (imide group), 1591, 1518, 1345, 1255, 1172, 1121, 808, 749 cm^{-1}. ^1H NMR ($CDCl_3$, δ 7.26 ppm): δ = 8.78 (2H, d, perylene H), 8.76 (2H, d, perylene H), 8.75 (2H, d, perylene H) and 8.71 (2H, d, perylene H); 7.70 (1H, t); 7.53 (2H, d); 7.47 (2H, d); 7.20 (2H, d); 3.06 (6H, s); 2.75 (2H, h); 1.19 (12H, d) ppm. ^{13}C NMR [$CDCl_3$ δ 77 ppm (3 peaks); *d*-TFA δ 162 ppm (4 peaks), 115 ppm (4 peaks)]: 166 (C=O), 164 (C=O), 122–145 (aromatic C), 47 (N-(CH_3)$_2$), 25 ($CH(CH_3)_2$), 23 ($CH(CH_3)_2$) ppm. DIP-mass: $[M]^{\bullet+}$ = 669 molecular ion peak was not observed, but 547 $[M]^{\bullet+}$ − Ph-$N(CH_3)_2$; 506 $[M]^{\bullet+}$ − Ph-$CH(CH_3)_2$; 490 $[M]^{\bullet+}$ − Ph-$CH(CH_3)_2$ − CH_3; 474 $[M]^{\bullet+}$ − Ph-$CH(CH_3)_2$ − $2CH_3$; 459 $[M]^{\bullet+}$ − Ph-$CH(CH_3)_2$ − $N(CH_3)_2$; 316 $[M]^{\bullet+}$ − $(CO)_2$N-Ph-$CH(CH_3)_2$ − Ph-$N(CH_3)_2$.

2.2. DNA preparation

The oligonucleotides were synthesized on a Thermo Electron DNA synthesizer and purified by reversed phase HPLC. DNAs were dissolved in a 70 mM potassium phosphate/100 mM potassium chloride/1 mM EDTA buffer at pH 6 (170 mM phosphate buffer). Phosphate buffer solution was prepared in a 95% H_2O/5% EtOH solution.

Following a standard procedure with small modifications [13,14] oligonucleotides were heated to 95 °C for 3 min and slowly cooled to room temperature. Two micromolar (μM) of each of the G-quadruplex structures was added to the solution of about 2 μM of the ligand at a total volume of 3 mL. Reaction mix-

Table 1
The visible absorption data of PYPER, ANPER, and DMANPER in solvents of different polarity (λ (nm), ε (L mol^{-1} cm^{-1}))

Solvent	ε[a]	Compound	λ_1	ε_1	λ_2	ε_2	λ_3	ε_3
Toluene	2.4	PYPER	460	9900	490	26400	527	39300
		ANPER	459	4900	490	12000	527	17530
		DMANPER	459	4630	490	11700	527	17500
Ethyl acetate	6.0	PYPER	454	12230	484	31400	519	46300
		ANPER	453	8200	483	18760	519	27200
		DMANPER	453	5000	483	12550	519	19000
Tetrahydrofuran	7.6	S1	456	21300	486	52000	522	56000
		S2	452	12170	482	31200	518	48000
		PYPER	456	9500	486	23800	522	34750
		ANPER	456	5800	485	13780	521	19850
		DMANPER	455	4320	486	11200	522	16900
Methanol	32.7	PYPER	457	14900	487	36900	523	54040
		ANPER	457	7500	488	18000	524	25500
		DMANPER	456	5300	488	13630	524	20400
Acetonitrile	35.9	PYPER	455	17680	486	39000	522	55900
		ANPER	454	8100	485	19600	520	28500
		DMANPER	455	7180	485	17450	521	25700
PBS buffer	80.2	PYPER	469	10900	501	17650	538	14300
		ANPER	469	10900	501	16400	538	14100
		DMANPER	468	8450	499	14040	534	11600

[a] Dielectric constant, ε, is taken from reference [39].

tures were incubated for 1–2 h at 37.2 °C. After the incubation, absorption spectra of the G-quadruplex-ligand complexes for all the nucleotides and ligands were compared to the nucleotide free solution (data not shown) of every ligands in phosphate buffer solution at pH 6.

3. Results and discussion

3.1. Stationary measurements, time-resolved experiments and fluorescence quantum yield determination studies

The absorption spectra of all the compounds in toluene show three vibronic maxima at 459, 490 and 527 nm. Large shoulder observed in the absorption spectra of the compounds at wavelength of 550 nm and longer indicates the non-fluorescent aggregates. The fluorescence spectra show emission maxima at 536 and 575 nm for ANPER and DMANPER and at 538 and 579 nm for PYPER in toluene. No considerable spectral shift or broadening can be observed upon varying the substituents of PDI dyes in solutions. Conformational or solvent relaxation does not occur for the compounds in the studied solvents.

We investigated the spectral characteristics of the compounds in five solvents of different polarity (Tables 1 and 2). In general, it is seen that higher the dielectric constants of the solvents, shorter the wavelengths of absorption and emission maxima of the compounds, excluding in methanol solution. This behavior may be attributed to the variation of dipole moments among the excited states and the ground states of unsymmetrical PDI dyes. Polarisibility of the excited states is lower than that of the ground states so that increasing solvent polarity stabilizes the ground states to a greater degree than the corresponding dipole moment in the excited states [40]. As a result, a hypsochromic shift is observed in polar solvents with respect to the less polar solvents.

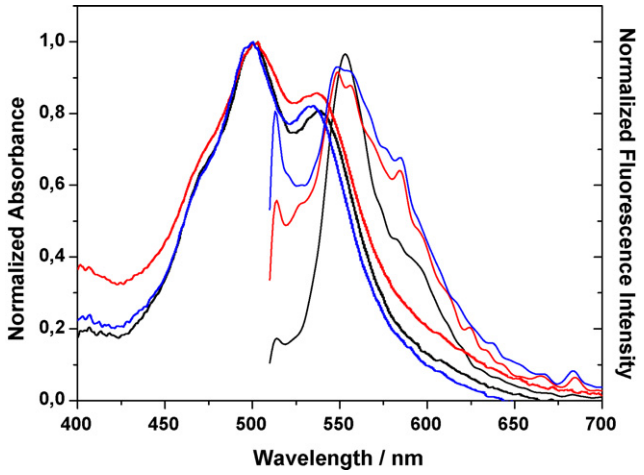

Fig. 1. The normalized visible absorption and fluorescence spectra of PYPER (black line), ANPER (red line) and DMANPER (blue line) in 170 mM phosphate buffer solution at pH 6 (λ_{exc} = 485 nm).

In methanol, an unexpected increase is observed at the absorption maxima of the compounds. This may be because hydrogen bonding ability of the compounds with solvent molecules in proton donating methanol solution stabilizes the charge-transfer excited state relative to the ground state. Because proton donating methanol interacts with the unshared valence electron pairs of the carbonyl group that will be the charge-transfer acceptor in the excited state. This may enhance charge-transfer by donating a partial positive charge into the functional group [40]. As a result the absorption spectrum is seen to shift to the long wavelength region. In addition, a strong red shift is observed for the studied compounds in 170 mM phosphate buffer solution at pH 6 (Fig. 1). In buffer solution, the absorption spectrum of PYPER displays maxima at 538 and 501 nm with a shoulder at 469 nm

Table 2
Fluorescence emission data, fluorescence quantum yields (Φ_F), radiative lifetimes (τ_0, ns), fluorescence lifetimes (τ_f, ns), fluorescence rate constants ($k_f \times 10^7$, s^{-1}), singlet energies (E_s, kcal mol^{-1}) and Stokes shifts ($\Delta\lambda$, nm) of PYPER, ANPER and DMANPER in solvents of different polarity (λ_{exc} = 485 nm)

Solvent	Compound	Φ_f	τ_0	τ_f	k_f	E_s	$\lambda_{em(max)}$	$\Delta\lambda$
Toluene	PYPER	0.81	10.6	8.5	9.4	55.0	538	53
	ANPER	0.13	30.4	3.9	3.3	55.0	536	51
	DMANPER	0.07	32.1	2.3	3.1	55.0	536	51
Ethyl acetate	PYPER	0.89	13.1	11.6	7.6	55.9	530	45
	ANPER	0.12	19.8	2.4	5.1	55.9	527	42
	DMANPER	0.06	33.4	2.0	3.0	55.9	529	44
Tetrahydrofuran	S1	0.91	10.3	9.4	9.7	55.6	533	48
	S2	0.87	10.7	9.3	9.3	56.0	529	44
	PYPER	0.84	14.6	12.2	6.8	55.6	532	47
	ANPER	0.11	24.8	2.7	4.0	55.7	530	45
	DMANPER	0.05	33.7	1.7	3.0	55.6	532	47
Methanol	PYPER	0.73	8.8	6.4	11.4	55.5	538	53
	ANPER	0.09	16.2	1.5	6.2	55.3	537	52
	DMANPER	0.05	24.8	1.2	4.0	55.3	538	53
Acetonitrile	PYPER	0.83	10.0	8.3	10.0	55.6	531	46
	ANPER	0.10	17.2	1.7	5.8	55.8	530	45
	DMANPER	0.05	23.0	1.2	4.3	55.7	532	47
PBS buffer	PYPER	<0.05	10.0	<0.05	10.0	57.9	553	68
	ANPER	<0.05	7.9	<0.05	12.7	57.9	552	67
	DMANPER	<0.05	11.8	<0.05	8.5	58.1	552	67

N-DODEPER was used as fluorescence standard (λ_{exc} = 485 nm, Φ_f = 1.0 in chloroform) [34].

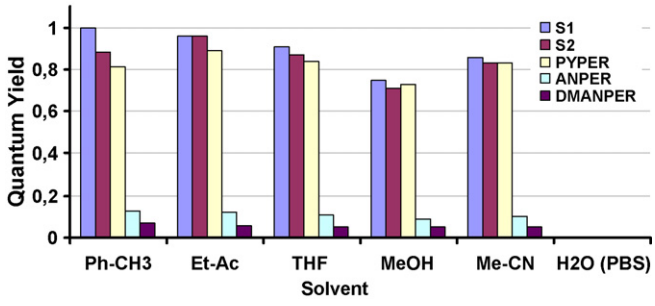

Fig. 2. Fluorescence quantum yields of PYPER, ANPER and DMANPER with respect to the model compounds S1 and S2 in five different solvents of increasing polarity and in 170 mM phosphate buffer at pH 6.

and gives a marked bathochromic shift (about 11 nm) in maxima compared to the same spectrum recorded in toluene. The fluorescence spectrum of PYPER shows a maximum at 538 nm in toluene, while the same spectrum displays a maximum at 553 nm in 170 mM phosphate buffer at pH 6. The absorption and emission spectra of both ANPER and DMANPER show similar long wavelength shifts in phosphate buffer at pH 6 and all the normalized absorption and emission spectra of the compounds in buffer solution are given in Fig. 1. While PYPER shows a marked shift of the emission maximum from 553 nm in phosphate buffer at pH 6 to 531 nm in acetonitrile, the corresponding change in DMANPER is much smaller. Contrary to the organic solvents, in phosphate buffer solution at pH 6, the emission spectra of the unsymmetrical PDIs are structureless. This may be attributed to the aggregation of the PDIs in phosphate buffer solution. Also, excited state relaxation of the unsymmetrical PDIs in phosphate buffer solution at pH 6, leads to an increase in dipole moment.

Quantum yields of fluorescence of PYPER, ANPER and DMANPER with respect to the model compounds S1 and S2 in five solvents of increasing polarity and in 170 mM phosphate buffer at pH 6 are compared in Fig. 2. Only a minor decrease or change is observed in organic solutions for all of the compounds. Fluorescence quantum yields of PYPER, ANPER and DMANPER are lower than that of the model compounds S1 and S2. A significant decrease of fluorescence quantum yields is observed for the unsymmetrical perylene diimides at about <0.05 in 170 mM phosphate buffer at pH 6. A striking observation is the very low fluorescence quantum yield values of ANPER and DMANPER in all of the organic solvents, $\Phi_f = 0.05$–0.13. Both of them have nitrogen atoms carrying non-bonding electron pairs, which initiate the quenching process in the perylene ring. Langhals and Jona have proved that a free amino group causes an intramolecular electron transfer to the HOMO level of the perylene chromophore, which diminishes the fluorescence [41,42].

Table 2 summarizes the photophysical properties of the studied compounds in five different solvents and in phosphate buffer solution. Fluorescence lifetimes are estimated from $\tau_f = \tau_0 \times \Phi_f$ and the rates of fluorescence are found from $k_f = 1/\tau_0$. The radiative lifetimes, τ_0, are calculated by the formula [43,44]: $\tau_0 = 3.5 \times 10^8/(\upsilon^2_{max} \times \varepsilon_{max} \times \Delta\upsilon_{1/2})$, where υ_{max} is the wavenumber, ε_{max} the molar extinction coefficient at the selected absorbance wavelength and $\Delta\upsilon_{1/2}$ is the half width of the selected absorbance in wavenumber unit. Fluorescence lifetimes of PYPER in solvents of different polarity are the highest among the other fluorescence lifetime values of unsymmetrical PDIs. Moreover, a slightly larger Stokes shift is observed in phosphate buffer solution with respect to organic solutions for unsymmetrical PDIs. This is attributed to the loss of vibration band structure of absorption and emission spectra of the studied compounds in water.

Table 3
Fluorescence decay times (τ_i, ns) and associated relative amplitudes (α_i) obtained by singular analysis for PYPER, ANPER and DMANPER in toluene (detected emission wavelength: 535 nm, time increment: 38 ps)

Compound	χ^2	τ_1	α_1 (%)	τ_2	α_2 (%)
PYPER	1.15	4.1	100	–	–
ANPER	1.12	3.9	89	0.8	11
DMANPER	1.18	3.9	92	1.1	8

Relative amplitude values, α_i, were calculated with the formula [45]: $W\alpha_i = \tau_i \times P_i/\Sigma\tau_i \times P_i$, where τ_i was the decay time of the compound and P_i was the number of free parameters in the fit function.

To investigate the excited state deactivation taking place in these molecules, time-resolved fluorescence measurements were undertaken. The fluorescence decay times of all the synthesized unsymmetrical PDIs were measured in toluene by the single photon counting method. Also, the results are given in Table 3. The analyses of the decays detected at emission wavelength of 535 nm reveal a mono-exponential decay at 4.1 ns for PYPER in toluene. This component is attributed to the stationary fluorescence of PDI. Combination of the fluorescence decay time and the fluorescence quantum yield of PYPER in toluene yields a fluorescence rate constant of $2 \times 10^8\ s^{-1}$. In contrast, the fluorescence decays of ANPER and DMANPER require bi-exponential decay to obtain good fit of the traces. The presence of two components in the fluorescence decay certainly suggests a multiple component system. The components at 0.8 ns (with amplitude of 11%) for ANPER and at 1.1 ns (with amplitude of 8%) for DMANPER can be attributed to the formation of excited state with more extensive conjugation between aniline group and PDI. The observed steady state emissions are mainly attributed to the state formed with 3.9 ns time constant for both the compounds. From the observed fluorescence quantum yields and the average decay components, the fluorescence rate constants of ANPER and DMANPER are found to be about 0.6×10^8, $0.3 \times 10^8\ s^{-1}$, respectively. These values indicate that both molecules have similar transition dipole moments and similar HOMO and LUMO energy levels. Fluorescence rate constants obtained for the relaxed conjugated states of ANPER and DMANPER are approximately 80% smaller than the fluorescence rate constant of PYPER. This means that the n orbital of the quencher lies above the HOMO of the PDI. Electron transfer from the non-bonding electron pair of the nitrogen atom to the ground state of the PDI explains the formation of charge-transfer.

3.2. Photo and thermal stabilities of the compounds

TGA curves of symmetrical PDI, perylene monoimide and three unsymmetrical PDIs are compared in Fig. 3. While the

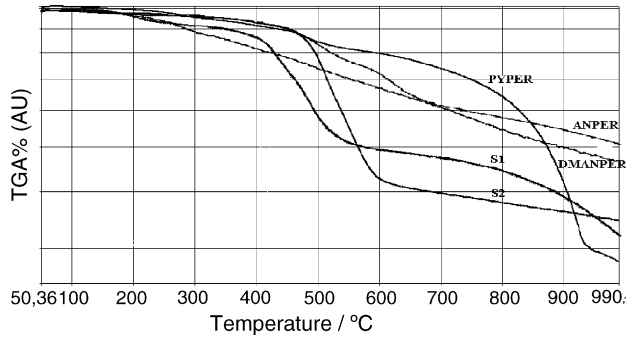

Fig. 3. TGA curves of PYPER, ANPER and DMANPER compared to the model compounds S1 and S2.

symmetrical one (S1) starts to loose weight at 481 °C, the unsymmetrical PDIs, PYPER, ANPER and DMANPER, start to loose weight at about 487, 488 and 290 °C, respectively. Moreover, perylene monoimide (S2) showed the most thermal stability with the decomposition temperature of 520 °C with respect to the other PDI derivatives. Therefore, one may conclude that the synthesized unsymmetrical PDIs except DMANPER are as stable as the symmetrical one. DMANPER has a dimethylamino group, which can be easily be degraded.

Photostability tests of all the synthesized compounds are determined under Xe lamp exposure in the fluorescence spectrophotometer in acetonitrile for 1 h. The compounds are excited at 254 nm and the data are acquired at the emission wavelength of 530 nm. Photodecomposition percents of the compounds are detected by monitoring the decrease in fluorescence intensity of the compounds. During the irradiation period, while emission intensities of S2 and PYPER increase, emission intensities of ANPER and DMANPER decrease (Fig. 4). Photodecompositions of the compounds are evaluated by the calculation of rate constant. The photodecomposition rate constants of the compounds are calculated with the formula [46], $\ln(I_0/I) = k_p \times t$, where I_0 and I are the emission intensities of the compound before and after the irradiation, respectively, k_p the photodecomposition rate constant and t is the irradiation time. k_p values of the S2, PYPER, ANPER and DMANPER are calculated to be 9.7×10^{-6}, 9.5×10^{-6}, 8.6×10^{-6} and $2.1 \times 10^{-5}\ s^{-1}$, respectively (Fig. 5). It is clearly seen that S1 and S2 are more resistant to UV radiation than the unsymmetrical PDIs. DMANPER is the least photoresistant compound. Highest photodecomposition rate for DMANPER is attributed to the presence of dimethyl amino moiety attached the perylene group that accelerates the degradation under UV radiation.

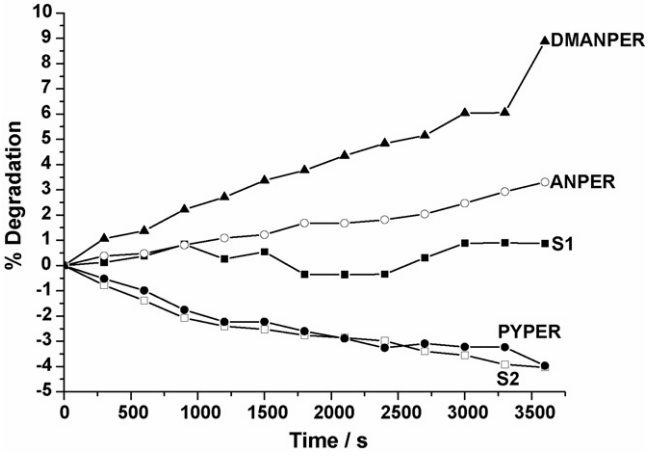

Fig. 4. Photodegradation (%) of PYPER, ANPER, DMANPER and the reference compounds S1 and S2 under Xe lamp exposure in the fluorescence spectrophotometer in MeCN at the excitation wavelength of 254 nm for 1 h ($\lambda_{emis} = 530$ nm).

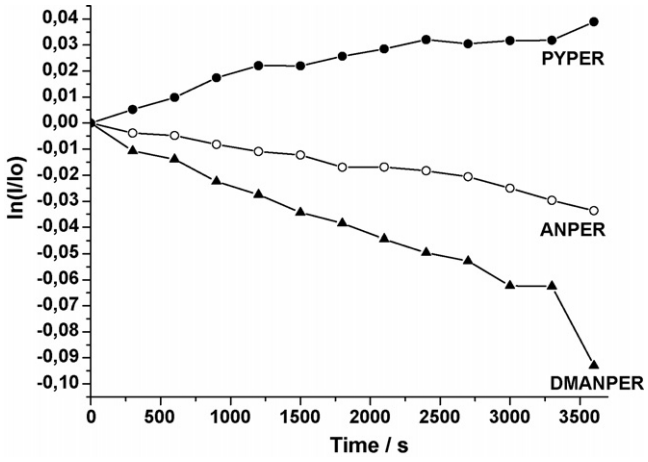

Fig. 5. Linear fits of the values obtained from the photodecomposition curves of PYPER, ANPER and DMANPER in MeCN solution (for PYPER: $9.5 \times 10^{-6}X + 0.00562$; R^2: 0.95, for ANPER: $8.6 \times 10^{-6}X + 0.000029$; R^2: 0.99 and for DMANPER: $2.1 \times 10^{-5}X + 0.00127$; R^2: 0.98).

3.3. G-quadruplex DNA binding selectivity

The ability to facilitate the formation of G-quadruplex DNA and the high binding selectivity to G4-DNA and G4′-DNA have been reported for various PDI derivatives including PIPER [28,30,47], Tel01 [28,30], Tel11 [29] and Tel12 [29]. Some of the PDI derivatives, which show aggregation behavior are suitable ligands to selective binding to G-quadruplex DNA. This aggregation-mediated selectivity of G-quadruplex ligands is very well known in the literature [30]. In our study, synthesized unsymmetrical PDI derivatives with diisopropyl side chains attached to the benzene ring show good solubility in different solvents and aggregation tendency in phosphate buffer solution at pH 6. Saturated concentrations of PYPER, ANPER and DMANPER in THF are 1.4×10^{-2}, 8.6×10^{-3} and 8.2×10^{-3} M, respectively. Both the loss of vibration band structure of absorption and emission spectra and also the low fluorescence quantum yields of the synthesized PDIs in phosphate buffer solution at pH 6 can be taken as evidences of aggregate formation of synthesized PDIs (Fig. 1).

In 170 mM phosphate buffer between pH 2 and 10, the absorption spectra of PYPER, ANPER and DMANPER are given in Fig. 6. pH changes do not effect the structure and the maxima of the absorption spectra of PYPER. However, for ANPER and DMANPER, the short wavelength shift and the loss of the structures of absorption spectra are observed with increasing values of pH. These changes may be attributed to the dissociation of

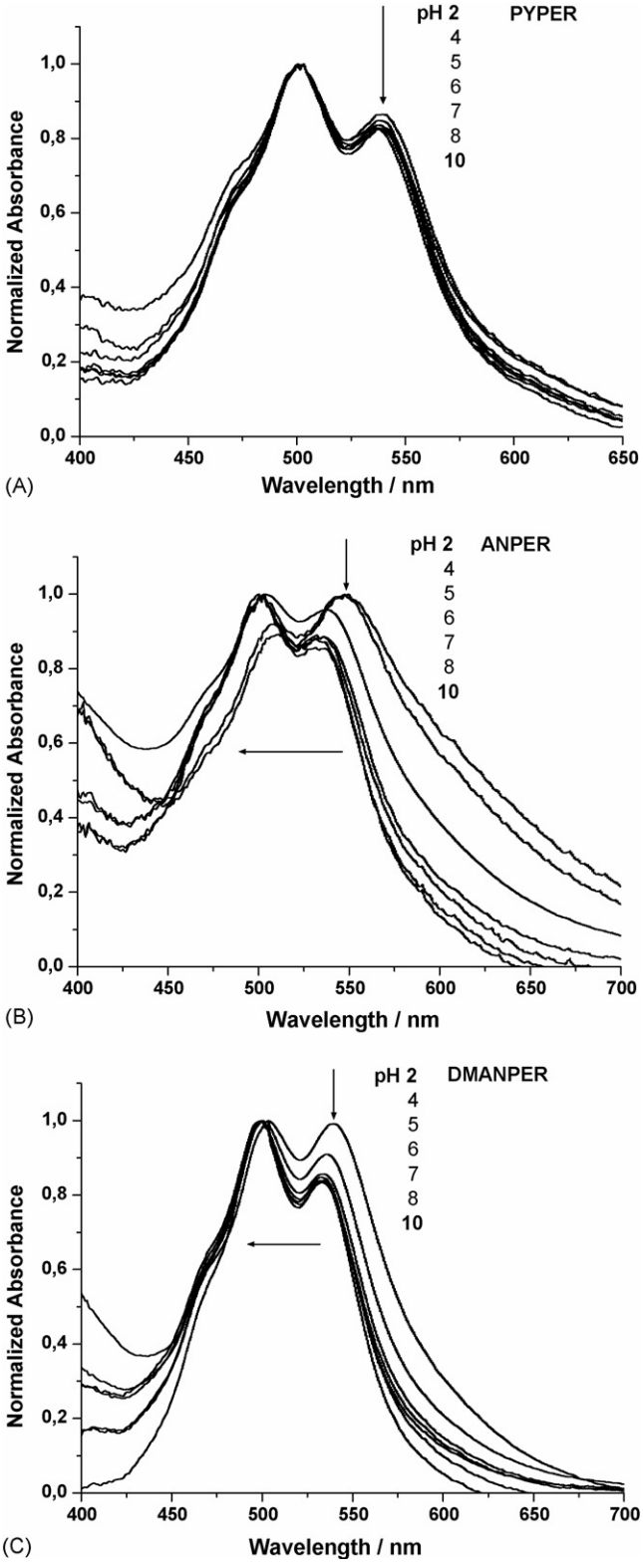

Fig. 6. Normalized absorption spectra of (A) PYPER, (B) ANPER and (C) DMANPER in 170 mM phosphate buffer at the indicated pH (concentration of each ligand is about 2 μM).

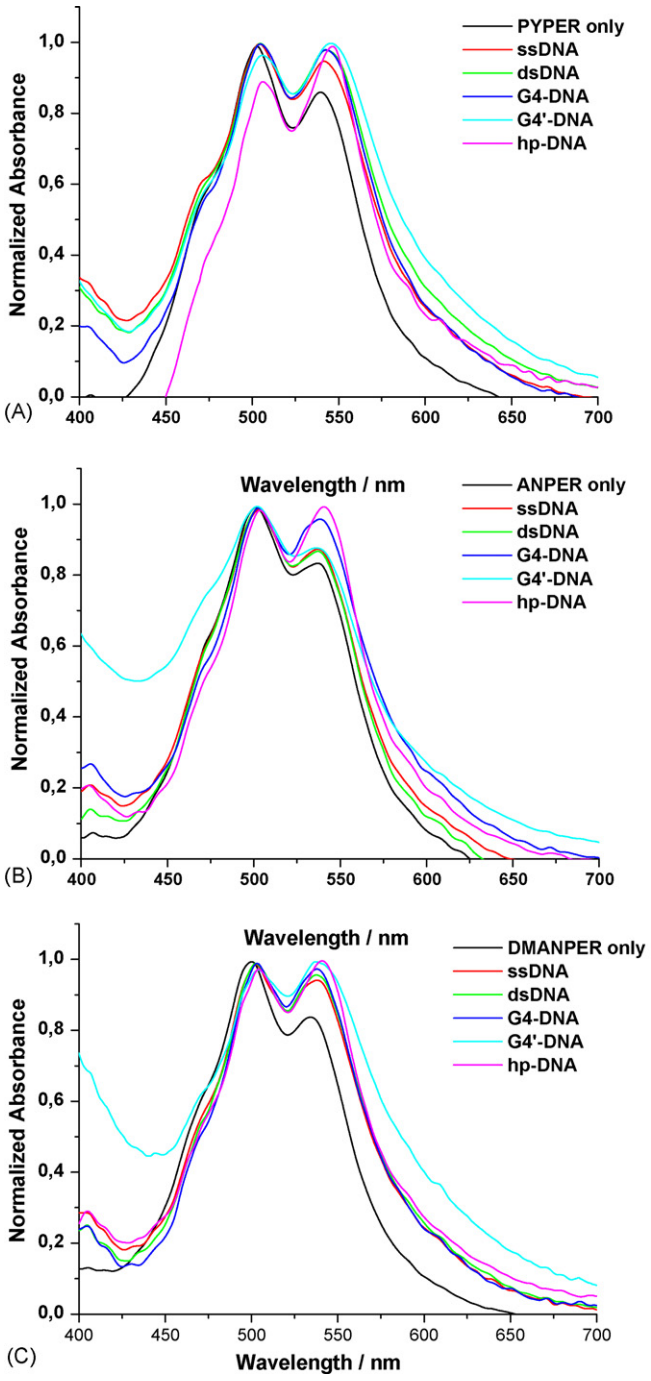

Fig. 7. Normalized absorption spectra of (A) PYPER, (B) ANPER and (C) DMANPER in a 70 mM potassium phosphate/100 mM potassium chloride/1 mM EDTA buffer at pH 6 (170 mM phosphate buffer) alone or in the presence of 1 equivalent of single-stranded DNA (ss-DNA) [d(TTTTTT)], double-stranded-DNA (ds-DNA) $[d(CGCGCGATATCGCGCG)]_2$, intermolecular G-quadruplex DNA (G4-DNA) $[d(TAGGGTTA)]_4$, intramolecular G-quadruplex DNA (G4′-DNA) $[d(TTAGGG)_4]$ or dimeric hairpin quadruplex DNA (hp-DNA) $[d(GGGGTTTTGGGG)]_2$ structure.

aggregated PDI molecules at lower pH values. These results are in agreement with the aggregation behavior of G-quadruplex DNA interactive perylene diimides reported earlier [28–30].

Fig. 7 shows the absorption spectra of the synthesized PDIs alone and interaction with the various DNA structures in 170 mM

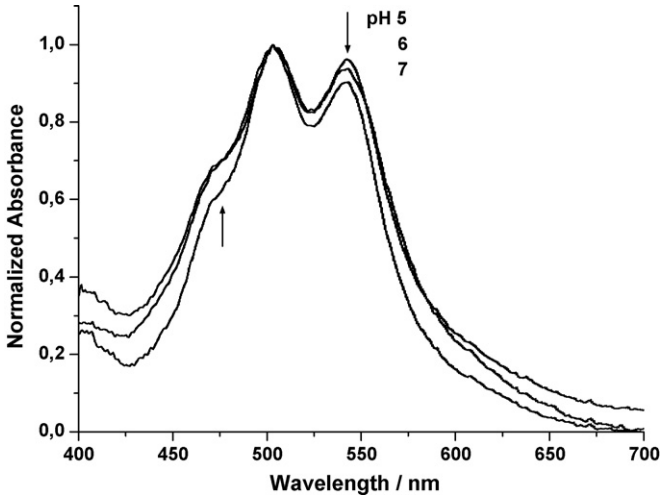

Fig. 8. Normalized absorption spectra of PYPER (2 μM) in 170 mM phosphate buffer in the presence of hp-DNA structure at the indicated pH.

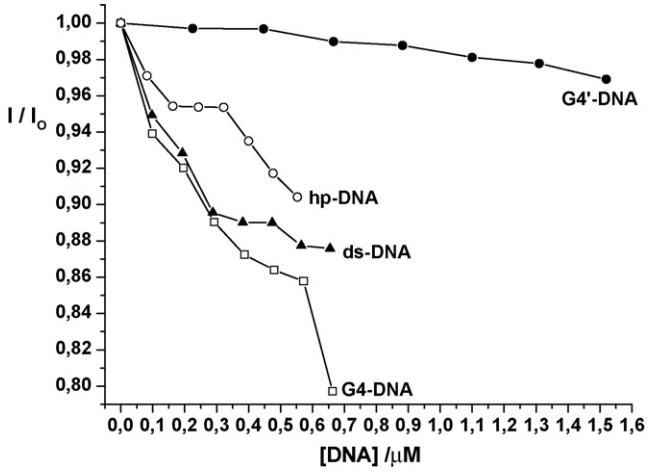

Fig. 9. Static quenching data of 2 μM of PYPER with double-stranded-DNA, intermolecular G-quadruplex DNA, intramolecular G-quadruplex DNA or dimeric hairpin quadruplex DNA structures in 170 mM phosphate buffer solution at pH 6 (λ_{exc} = 490 nm).

phosphate buffer solution at pH 6. More gradual red shifts from 501 to 505 nm and 538 to 545 nm are observed for PYPER in the presence of G4′-DNA. The peak-to-valley ratio for 0–0 transition at 545 nm increases from 1.13 in the absence of G4′-DNA to 1.33 in the presence of G4′-DNA. These data can be taken as proof that some stacking interactions occur between PYPER and the G4′-DNA structure in phosphate buffer solution at pH 6. We observe significant bathochromic shifts from 499 to 503 nm and 534 to 539 nm for DMANPER in the presence of G4′-DNA. These data for perylene diimides interacting with different forms of G-quadruplex structures are in agreement with the data given in literature [28–30]. Similar red shifts are observed for PIPER, Tel01, Tel11 and Tel12. All these data suggest that synthesized PDIs interact and bind to a specific side of DNA.

The aggregation behavior of PYPER interacting with hp-DNA in 170 mM phosphate buffer solution was investigated at different pH values (Fig. 8). Higher the pH of the buffer solution, the more increase in the aggregated state of PYPER.

3.4. Fluorescence quenching of unsymmetrical PDIs with nucleotides

PDIs are known to be both electron acceptors and electron donors in the literature [48,49]. In order to confirm that unsymmetrical PDI ligands interact with nucleotides, fluorescence quenching of PYPER, ANPER and DMANPER were studied at increasing concentrations of different DNA structures. Approximately, 0.1–1.5 μM solutions of each nucleotides was added to solutions of unsymmetrical PDI derivatives, which were dissolved in 70 mM potassium phosphate/100 mM potassium chloride/1 mM EDTA buffer at pH 6. Fluorescence emission is detected after equilibrium has been reached to an optimum level (5–10 min).

Fig. 9 shows that PYPER is easily bound to the ds-DNA, G4-DNA and hp-DNA. PYPER interacts with little affinity, but high selectivity for the G4′-DNA structure. It shows about 9.3-fold selectivity for binding to G4′-DNA versus double-stranded DNA base pairs. Table 4 gives information about the concentration of DNA required to decrease the initial fluorescence intensity of PDI ligands by 50% in the quenching experiments in phosphate buffer at pH 6. Marked enhancements of ANPER and DMANPER emissions are observed with the addition of nucleotides. These enhancements can be explained by the changes in the stability constant of PDI aggregates. When the stability constant of PDI aggregates is less favorable than the association constant of PDI-nucleotide binding, fluorescence enhancement can be observed. In this interaction, PDI ligands are most likely to be monomeric or dimeric forms. ANPER is a more pH-sensitive ligand than the other studied ligands (see Fig. 6). The ligand can be easily changed from aggregate state to the monomeric form. For this reason, a significant enhancement of fluorescence emission is observed at very low concentrations of nucleotides. While ANPER emission is enhanced at about 15% in the presence of 0.55×10^{-6} M ss-DNA, the corresponding change in the presence of G4′-DNA at the same concentration is only about 2% (data not shown). This little enhancement in emission intensity can be exploited for good binding selectivity of ANPER to G4′-DNA. This result supports the aggregation-mediated selectivity of binding between ANPER and the G-quadruplex formed in the G4′-DNA structure. As indicated in Table 4, DMANPER also shows good binding selectivity to G-quadruplex formed in G4′-DNA structure. DMANPER displays about a 4.9-fold selectivity for binding G4′-DNA versus intermolecular G-quadruplex DNA.

Table 4
Concentration of DNA ($\times 10^{-6}$ M) required to decrease the initial fluorescence intensity of PYPER, ANPER and DMANPER ligands by 50% in the quenching experiments in phosphate buffer at pH 6

DNA structure	PYPER	ANPER	DMANPER
ds-DNA	2.73	2.72	nq[a]
G4-DNA	1.88	nq[a]	2.97
G4′-DNA	25.42	nq[a]	14.61
hp-DNA	3.26	nq[a]	nq[a]

[a] Not quenched.

Table 5
Fluorescence quenching rate constants, k_q ($\times 10^{12}\,M^{-1}\,s^{-1}$), of PYPER, ANPER and DMANPER ligands interacting with different DNA structures in quenching experiments in phosphate buffer at pH 6

DNA structure	PYPER	ANPER	DMANPER
ds-DNA	9.43	16.21	nq[a]
G4-DNA	14.80	nq[a]	4.38
G4′-DNA	0.95	nq[a]	0.86
hp-DNA	7.81	nq[a]	nq[a]

[a] Not quenched.

These results indicate that all of the studied ligands show a good binding affinity, but little selectivity for ss-DNA, ds-DNA, G4-DNA and hp-DNA, which may be attributed to stacking of the dye along the DNA polymer. Charge–charge effects between the positively charged ligands (at pH 6) and negatively charged polyanionic backbone of the DNA generate the rapid initial binding in 5 or 10 min. Therefore, ligands aggregate on the polymeric backbone of the DNAs. A striking result of this study is the G4′-DNA binding selectivity of the synthesized ligands. The possible binding type of the ligands for the G4′-DNA is the end-stacking interactions, which need only one face of PDIs to interact with G4′-DNA tetrads. Ligand aggregation may facilitate the binding selectivity to G-quadruplex formed in G4′-DNA structure.

For evaluating the quenching dynamics, the steady-state fluorescence quenching results of unsymmetrical PDIs with nucleotides are analyzed following the Stern–Volmer equation [50],

$$\frac{I_0}{I} = 1 + k_q \times \tau_0 \times [Q],$$

where I_0 and I are the fluorescence intensities in the absence and presence of quenchers, respectively, and k_q the quenching constant and τ_0 is the radiative lifetime in the absence of the quencher. Fluorescence quenching rate constants of PDIs interacting with different DNA structures are given in Table 5. Calculated quenching rate constant values of 10^{11}–$10^{13}\,M^{-1}\,s^{-1}$ are above the limit of diffusion controlled quenching rates of $10^{10}\,M^{-1}\,s^{-1}$ and indicates almost static quenching [51]. Condensation of the PDIs onto the DNA strands with the increasing concentration of G-quadruplex DNAs initiates the self-quenching process. Fluorescence emissions of the PDIs decrease. Higher quenching rate constants support the charge–charge effects of the PDIs with the polyanionic backbone of the DNA. k_q values for PYPER and DMANPER interacting with G4′-DNA are calculated to be about 0.95×10^{12} and $0.86 \times 10^{12}\,M^{-1}\,s^{-1}$, respectively. These values may support the claim for self quenching of the PDIs which aggregate on the polymeric structure of the DNAs.

4. Conclusions

In this study, we have synthesized new unsymmetrical PDIs, *N*-(2, 6-diisopropylphenyl)-*N*′-(4-pyridyl)- perylene-3, 4, 9, 10-tetracarboxylic diimide (PYPER), *N*-(2,6-diisopropylphenyl)-*N*′-(4-aminophenyl)-perylene-3,4,9,10-tetracarboxylic diimide (ANPER) and *N*-(2,6-diisopropylphenyl)-*N*′-[4-(*N*,*N*-dimethylaminophenyl)]-perylene-3,4,9,10-tetracarboxylic diimide (DMANPER) to investigate their binding selectivity to the G-quadruplex DNA structure. Photophysical properties of these compounds in five solvents of different polarity and in phosphate buffer solution have been compared. These compounds showed good solubility in organic solvents and aggregation tendency in phosphate buffer solution at pH 6. Time-resolved measurements have indicated that more extensive conjugation between the aniline moiety and PDI in the excited state of ANPER and DMANPER gives two decay components.

Both absorption binding and fluorescence quenching experiments of unsymmetrical PDI ligands with different nucleotides have demonstrated that these ligands bind to G-quadruplex DNA. Binding selectivity of these PDIs to G-quadruplex DNA has been examined with fluorescence quenching experiments. The studied ligands have shown good binding selectivity to G-quadruplex. Among the studied compounds, PYPER is found to be the most selective interactive ligand for G-quadruplex, formed in the G4′-DNA structure. PYPER has been successfully radioiodinated with ^{131}I. Scintigraphic imaging with the radioiodinated compound (^{131}I-PYPER) has been performed on rats. It has been found that ^{131}I-PYPER has diagnostic and therapeutic application potentials in nuclear medicine [52]. These results have shown that unsymmetrical PDI ligands offer promising molecular architectures for the design of new G-quadruplex DNA-interactive ligands based on PDI structure with therapeutic application potentials in nuclear medicine.

Acknowledgements

We acknowledge the project support funds provided by the Research Center of Ege University (EBILTEM), Research Council of Celal Bayar University (BAP), Alexander von Humboldt Foundation (AvH) and the State Planning Organization of Turkey (DPT). We thank to Özgül Haklı for providing mass analyses and to Dr. Stephen Thomas Astley for the proof reading.

References

[1] P.R.L. Malenfant, C.D. Dimitrakopoulos, J.D. Gelorme, L.L. Kosbar, T.O. Graham, A. Curioni, W. Andreoni, Appl. Phys. Lett. 80 (2002) 2517–2519.
[2] D. Schlettwein, D. Wöhrle, E. Karmann, U. Melville, Chem. Mater. 6 (1994) 3–6.
[3] S. Ferrere, A. Zaban, B.A. Gregg, J. Phys. Chem. B 101 (1997) 4490–4493.
[4] L. Schmidt-Mende, A. Fechtenkötter, K. Müllen, E. Moons, R.H. Friend, J.D. MacKenzie, Science 293 (2001) 1119–1122.
[5] M. Sadrai, L. Hadel, R.R. Sauers, S. Husain, K. Krogh-Jespersen, J.D. Westbrook, G.R. Bird, J. Phys. Chem. 96 (1992) 7988–7996.
[6] K.-Y. Law, Chem. Rev. 93 (1993) 449–486.
[7] P. Ranke, I. Bleyl, J. Simmerer, D. Haarer, A. Bacher, H.W. Schmidt, Appl. Phys. Lett. 71 (1997) 1332–1334.
[8] M.J. Fuller, C.J. Walsh, Y. Zhao, M.R. Wasielewski, Chem. Mater. 14 (2002) 952–953.
[9] S. Becker, A. Böhm, K. Müllen, Chem. Eur. J. 6 (2000) 3984–3990.
[10] K.D. Belfield, M.V. Bondar, O.V. Przhonska, K.J. Schafer, J. Photochem. Photobiol., A 151 (2002) 7–11.
[11] H. Dincalp, S. Icli, J. Photochem. Photobiol., A 141 (2001) 147–151.
[12] F. Yukruk, A.L. Dogan, H. Canpinar, D. Guc, E.U. Akkaya, Org. Lett. 7 (2005) 2885–2887.

[13] O.Y. Fedoroff, M. Salazar, H. Han, V.V. Chemeris, S.M. Kerwin, L.H. Hurley, Biochemistry 37 (1998) 12367–12374.
[14] H. Han, C.L. Cliff, L.H. Hurley, Biochemistry 38 (1999) 6982–6986.
[15] H. Han, R.J. Bennett, L.H. Hurley, Biochemistry 39 (2000) 9311–9316.
[16] N.W. Kim, M.A. Piatyszek, K.R. Prowse, C.B. Harley, M.D. West, P.L.C. Ho, G.M. Coviello, W.E. Wright, R.L. Weinrich, J.W. Shay, Science 266 (1994) 2011–2015.
[17] J. Lingner, T.R. Hughes, A. Shevchenko, M. Mann, V. Lundblad, T.R. Cech, Science 276 (1997) 561–567.
[18] T.M. Nakamura, G.B. Morin, K.B. Chapman, S.L. Weinrich, W.H. Andrews, J. Lingner, C.B. Harley, T.R. Cech, Science 277 (1997) 955–959.
[19] D. Sun, B. Thompson, B.E. Cathers, M. Salazar, S.M. Kerwin, J.O. Trent, T.C. Jenkins, S. Neidle, L.H. Hurley, J. Med. Chem. 40 (1997) 2113–2116.
[20] G. Laughlan, A.I.H. Murchie, D.G. Norman, M.H. Moore, P.C.E. Moody, D.M.J. Lilley, B. Luisi, Science 265 (1994) 520–524.
[21] D.E. Gilbert, J. Feigon, Curr. Opin. Struct. Biol. 9 (1999) 305–314.
[22] H. Arthanari, S. Basu, T.L. Kawano, P.H. Bolton, Nucleic Acids Res. 26 (1998) 3724–3728.
[23] I. Hag, J.O. Trent, B.Z. Chowdhry, T.C. Jenkins, J. Am. Chem. Soc. 121 (1999) 1768–1779.
[24] M.A. Read, S. Neidle, Biochemistry 39 (2000) 13422–13432.
[25] S.M. Kerwin, D. Sun, J.T. Kern, A. Rangan, P.W. Thomas, Bioorg. Med. Chem. Lett. 11 (2001) 2411–2414.
[26] P. Alberti, P. Schmitt, C.-H. Nguyen, C. Rivalle, M. Hoarau, D.S. Grierson, J.-L. Mergny, Bioorg. Med. Chem. Lett. 12 (2002) 1071–1074.
[27] W. Tuntiwechapikul, J.T. Lee, M. Salazar, J. Am. Chem. Soc. 123 (2001) 5606–5607.
[28] S.M. Kerwin, G. Chen, J.T. Kern, P.W. Thomas, Bioorg. Med. Chem. Lett. 12 (2002) 447–450.
[29] J.T. Kern, S.M. Kerwin, Bioorg. Med. Chem. Lett. 12 (2002) 3395–3398.
[30] J.T. Kern, P.W. Thomas, S.M. Kerwin, Biochemistry 41 (2002) 11379–11389.
[31] M. Franceschin, A. Alvino, G. Ortaggi, A. Bianco, Tetrahedron Lett. 45 (2004) 9015–9020.
[32] M.A. Abdalla, J. Bayer, J.O. Rädler, K. Müllen, Angew. Chem. Int. Ed. 43 (2004) 3967–3970.
[33] L. Rossetti, M. Franceschin, S. Schirripa, A. Bianco, G. Ortaggi, M. Savino, Bioorg. Med. Chem. Lett. 15 (2005) 413–420.
[34] S. Icli, H. Icil, Spectrosc. Lett. 29 (1996) 1253–1257.
[35] J.R. Knutson, J.M. Beechem, L. Brand, Chem. Phys. Lett. 102 (1983) 501–507.
[36] D.V. O'Connor, D. Phillips (Eds.), Time-Correlated Single Photon Counting, Academic Pres, London, 1984, pp. 252–287.
[37] M. Thelakkat, P. Pösch, H.-W. Schmidt, Macromolecules 34 (2001) 7441–7447.
[38] L.D. Wescott, D.L. Mattern, J. Org. Chem. 68 (2003) 10058–10066.
[39] J.C. Scaiano (Ed.), CRC Handbook of Organic Photochemistry, vol. II, CRC Pres, Inc., Florida, 1989, p. 344.
[40] P. Suppan (Ed.), Chemistry and Light, The Royal Society of Chemistry, London, 1994, pp. 77–86.
[41] H. Langhals, W. Jona, Chem. Eur. J. 4 (1998) 2110–2116.
[42] L. Zang, R. Liu, M.W. Holman, K.T. Nguyen, D.M. Adams, J. Am. Chem. Soc. 124 (2002) 10640–10641.
[43] P. Suppan (Ed.), Chemistry and Light, The Royal Society of Chemistry, London, 1994, pp. 60–62.
[44] N.J. Turro (Ed.), Molecular Photochemistry, Benjamin, London, 1965, pp. 48–50.
[45] M. Maus, R. De, M. Lor, T. Weil, S. Mitra, U.-M. Wiesler, A. Herrmann, J. Hofkens, T. Vosch, K. Müllen, F.C. de Schryver, J. Am. Chem. Soc. 123 (2001) 7668–7676.
[46] L. Moeini-Nombel, S. Matsuzawa, J. Photochem. Photobiol., A 119 (1998) 15–23.
[47] L. Rossetti, M. Franceschin, A. Bianco, G. Ortaggi, M. Savino, Bioorg. Med. Chem. Lett. 12 (2002) 2527–2533.
[48] S. Icli, S. Demiç, B. Dindar, A.O. Doroshenko, C. Timur, J. Photochem. Photobiol., A 136 (2000) 15–24.
[49] H. Icil, Spectrosc. Lett. 31 (1998) 747–755.
[50] J.R. Lakowicz (Ed.), Principles of Fluorescence Spectroscopy Part 8, Kluwer Academic/Plenum Publisher, New York, 1999, pp. 239–242.
[51] G.J. Kavarnos, N.J. Turro, Chem. Rev. 86 (1986) 401–449.
[52] U. Avcıbaşı, H. Dinçalp, T. Ünak, Y. Yıldırım, N. Avcıbaşı, Y. Duman, S. İçli, J. Radioanal. Nucl. Chem., in press.